

miR-22-3p enhances multi-chemoresistance by targeting NET1 in bladder cancer cells

JUN XIAO^{1*}, SANQIANG NIU^{2*}, JIAHONG ZHU^{2*}, LEI LV³, HUI DENG³, DAQING PAN¹, DEYUN SHEN¹, CONGYUN XU¹, ZHOU SHEN¹ and TAO TAO¹

¹Department of Urology, Anhui Provincial Hospital, The First Affiliated Hospital of University of Science and Technology of China, Hefei, Anhui 230001; ²Department of Urology, Bozhou People's Hospital, Bozhou, Anhui 236800; ³Cancer Epigenetics Program, Anhui Cancer Hospital, The First Affiliated Hospital of University of Science and Technology of China, Hefei, Anhui 230031, P.R. China

Received October 22, 2017; Accepted March 13, 2018

DOI: 10.3892/or.2018.6355

Abstract. With the discovery of new chemotherapeutic drugs, chemotherapy becomes increasingly valuable. However, the resistance of tumor cells to chemotherapeutic agents significantly limits the effectiveness and causes chemotherapy failure. MicroRNAs have been shown to regulate drug resistance in many types of cancer. In the present study, we measured the chemosensitivity of five bladder cancer (BCa) cell lines to seven commonly used chemotherapeutic drugs by Vita-Blue assay. We then identified the most sensitive (5637) and most tolerant cell lines (H-bc) and conducted a multi-group test. This test included expression group analyses of coding and non-coding genes (miR-omic and RNA-seq). Based on our analyses, we selected miR-22-3p as a target. We then determined its own target gene [neuroepithelial cell transforming 1 (NET1)] by bioinformatic analysis and confirmed this finding by TaqMan-quantitative reverse transcription polymerase chain reaction (qRT-PCR), western blot analysis and luciferase reporter assay. The effect of miR-22-3p on BCa multi-chemoresistance was also determined by transfecting cells with the miR-22-3p-mimic or miR-22-3p-antagomiR. We assessed the involvement of NET1 in BCa chemoresistance by siRNA-mediated NET1 inhibition or pINDUCER21-enhanced green fluorescent protein-NET1-mediated overexpression. Plate colony formation and apoptosis assays were conducted to observe the effects of miR-22-3p and NET1 on BCa chemoresistance. In conclusion, our results suggest that

miR-22-3p promotes BCa chemoresistance by targeting NET1 and may serve as a new prognostic biomarker for BCa patients.

Introduction

Bladder cancer (BCa) is the second most common malignant tumor of the urogenital system and has the fourth highest incidence among all tumors diagnosed in males in Western countries (1). Local perfusion chemotherapy can significantly reduce the recurrence rate in patients with non-muscle-invasive BCa. However, nearly half of patients still experience tumor recurrence and metastasis after the second round of chemotherapy (2). Muscle-invasive BCa is also resistant to chemotherapeutic drugs and often progresses with poor prognosis. Although different patients exhibit varying sensitivities to chemotherapy drugs, BCa is resistant to multiple drugs in most cases. These resistance characteristics significantly influence the effectiveness of clinical chemotherapy (3). Therefore, elucidating the mechanisms involved in the chemoresistance of BCa has become increasingly urgent.

MicroRNAs (miRNAs) are endogenous single-stranded, small-molecule non-coding RNAs with lengths of 19-25 nucleotides (4). These molecules participate in the regulation of cell formation, differentiation, proliferation, apoptosis and other basic biological processes. miRNAs bind to the 3' untranslated region (3'UTR) of target mRNAs as completely or incompletely complementary pairs and cause mRNA degradation or protein expression inhibition. Ultimately, target gene processes are negatively regulated (5). By regulating different downstream target genes, miRNAs participate in a wide range of key signaling pathways, such as the DNA damage, Notch and nuclear factor (NF)- κ B pathways, and consequently affect mechanisms of tumor cell chemoresistance. As such, miRNAs serve as promising candidate molecular markers (6). For example, in BCa, various miRNAs, including miR-34a (7), miR-21 (8), miR-30d, miR-181, miR-199a-5p (9) and miR-193a-3p, are reportedly associated with chemoresistance (10-13).

miR-22-3p is located on chromosome 17 (17p13.3) and is adjacent to the p53 gene (14). Recent studies have shown that miR-22-3p plays a vital role in different types of cancer,

Correspondence to: Dr Tao Tao, Department of Urology, Anhui Provincial Hospital, The First Affiliated Hospital of University of Science and Technology of China, 17 Lujiang Road, Hefei, Anhui 230001, P.R. China
E-mail: taotao860721@126.com

*Contributed equally

Key words: miR-22-3p, neuroepithelial cell transforming 1, multi-chemoresistance, bladder cancer

including breast, rectal, pancreatic, hepatocellular (15) and gastric cancers (16). As a potent proto-oncogenic miRNA, miR-22 is noted for its role in chromatin remodeling. miRNAs were found to trigger epithelial-mesenchymal transition, enhance stemness and promote breast cancer development and metastasis in mouse models by increasing methylation of the miR-200 promoter. This process suppressed expression of the anti-metastatic miR-200 family (17). In hematological malignancies, miR-22 was also reported to reduce global levels of 5-hydroxymethylcytosine (5-hmC) in the genome. 5-hmC was found to trigger an increase in cell self-renewal capability and defective differentiation and tumorigenesis by targeting tet methylcytosine dioxygenase 2 (18). miR-22 has also been noted to promote tumorigenesis by suppressing expression of phosphatase and tensin homolog (PTEN) in prostate cancer (19). However, some *in vitro* studies have revealed the tumor-suppressor functions of miR-22; these functions included restraining invasion and metastasis of hepatocellular carcinoma by inhibiting expression of cluster of differentiation (CD)147 (20), CD151 (gastric cancer) (16) and lysine-specific demethylase 3A (KDM3A) (Ewing's sarcoma) (21). In osteosarcoma, expression of high mobility group box protein 1 (HMGB1), a direct target of miR-22, and subsequent HMGB1-mediated autophagy were found to be upregulated and to contribute to chemotherapy resistance *in vitro*. However, as a compensatory effect, miR-22 is presumably upregulated during chemotherapy (22).

In the present study, we performed miR-omic and RNA-seq assays and discovered differentially expressed genes in multi-drug chemosensitive (5637) and multi-drug chemoresistant (H-bc) BCa cell lines. Additional in-depth studies demonstrated that miR-22-3p promoted chemoresistance in BCa by inhibiting the neuroepithelial cell transforming 1 (NET1) gene, a target gene of miR-22-3p that is a RhoA guanine exchange factor, via cysteine residues in its membrane domain, which mediates extracellular signal transduction and is also associated with tumor invasion, metastasis and chemoresistance (23,24). We also further revealed the role of NET1 and miR-22a-3p in multi-drug chemotherapy of BCa by plate colony formation assay and apoptotic experiments.

Materials and methods

Cell culture and reagents. Five BCa cell lines were purchased from the Chinese Academy of Cell Resource Centre (Shanghai, China). These cell lines included 5637 (ATCC No. HTB-9), T24 (ATCC No. HTB-4), Um-Uc-3 (ATCC No. CRL-1749), J82 (ATCC No. HTB-1) and H-bc (established by the Cancer Research Institute of Kunming Medical College in 1986). The Um-Uc-3 cell line was cultured in Minimum Essential Medium (MEM; Invitrogen; Thermo Fisher Scientific, Inc., Waltham, MA, USA) + 10% fetal bovine serum (FBS; Invitrogen; Thermo Fisher Scientific, Inc.) and 1% glutamine at 37°C in 5% CO₂. The remaining cell lines were cultured in Roswell Park Memorial Institute (RPMI)-1640 medium (Invitrogen; Thermo Fisher Scientific, Inc.) + 10% FBS and 1% glutamine at 37°C in 5% CO₂. miR-22-3p mimic and antagomiR, NET1 siRNA, scrambled sequences (including mimic-negative control (NC), antagomiR-NC and siRNA-NC) and the riboFECT CP Transfection kit were supplied by

Guangzhou Ribobio Co., Ltd. (Guangzhou, China). Control check (CK) represents the use of cell culture media only. pINDUCER21 was provided by Professor Yang Wang (Dalian Medical University, Dalian, China).

pINDUCER21-enhanced green fluorescent protein (EGFP)-NET1 construction. pINDUCER21-EGFP and OmicsLink full-length open reading frame (ORF) (GeneCopoeia, Rockville, MD, USA) expression clone plasmid (NET1) were transformed into DH5α *Escherichia coli* cells for DNA amplification and extraction. OmicsLink full-length ORF of NET1 was digested with restriction endonucleases *Hind*III and *Xho*I. Then, small fragments (insert) were recovered after digestion (1.7 kb), and ends were reinforced. pINDUCER21-EGFP plasmid was digested as a vector via restriction endonucleases *Mlu*I and Klenow. The insert was then ligated into a new expression vector by T4 DNA ligase, and ligation products were used to transform DH5α *E. coli* bacteria. Positive clones pINDUCER21-EGFP-NET1 were screened for resistance to ampicillin. Then, plasmids were extracted by Gel Recovery kit (Omega Bio-tek, Inc., Norcross, GA, USA) and verified by restriction enzyme digestion. Finally, the correct clone was selected for sequencing.

Luciferase reporter assay. The 3'UTR fragment of NET1 (range=chr10:5498958-5500183) was amplified with primers NET1 UTR sense 5'-GCGCTAGCAGAAGGCTCTGTGTGT TAACTGAT-3' and NET1 UTR antisense 5'-GCGGATATC TTCCATCTTATGACTAAATCCACC-3'. Polymerase chain reaction (PCR) products were cloned into a firefly luciferase reporter vector pGL3-control (Invitrogen; Thermo Fisher Scientific, Inc.) termed as pGL3-Luc-NET1-3'UTR-wt. The plasmid carrying the mutated sequence for the seed region of miR-22-3p in complementary sites (range=chr10:5499107-5499114) was generated based on the pGL3-NET1-3'UTR plasmid by primer design for point-directed mutagenesis experiments. This plasmid was designated as pGL3-Luc-NET1-3'UTR-mut. Plasmids were confirmed by sequencing analysis. Cells were seeded into 96-well plates at 1x10⁴ cells/well and transfected with a mixture of 50 ng pGL3-luc-NET1-wt/mut, 5 ng *Renilla* and 15 pmol antagomiR or unrelated control (NC) oligo nucleotides by using the riboFECT CP transfection kit in accordance with the manufacturer's instructions. Firefly and *Renilla* luciferase activities were measured 18 h after transfection by the Dual-Luciferase Reporter Assay system (Promega, Madison, WI, USA) through a Promega GloMax 20/20 luminometer (Promega).

Chemoresistance studies. Clinical-grade pirarubicin (Pi; Shenzhen Wanle Pharmaceutical Co., Ltd., Shenzhen, China), paclitaxel (Pa; Taiji Pharmaceutical Co., Ltd., Sichuan, China), adriamycin (Ad; Pfizer, Suzhou, China), epirubicin hydrochloride (EH; Zhejiang Haizheng Co., Ltd., Zhejiang, China), hydroxycamptothecin (Hy; Lishizhen Pharmaceutical Co., Ltd., Wuhan, China), cisplatin (Ci; Haosen Pharmaceutical Co., Ltd., Jiangsu, China) and gemcitabine (Ge; Dihao Pharmaceutical Co., Ltd., Jiangsu, China) (NCI Dictionary of Cancer Terms, <http://www.cancer.gov/dictionary>) were used in the present study. Cells in the logarithmic growth phase were seeded in triplicate in 96-well plates at a density

of 0.4×10^4 cells/well and treated with the dose of the agents required for inhibition of 50% of the cells (IC_{50}) at 72 h. Cell survival was then measured by Vita-Blue (Biotool LLC, Houston, TX, USA; B34102; Ex 530-570 nm/Em 590-620 nm reading)-based cell proliferation assay. Relative survival was presented as the percentage relative to the results in the control group (no drugs added).

Cell proliferation assay. Cells in the logarithmic growth phase were seeded in 96-well plates at a cell density of 0.2×10^4 cells/well (in triplicate) to allow adhesion. At 0, 24, 48, 72 and 96 h, Vita-Blue-based cell density assays were performed. Cells were incubated with 5 μ l Vita-Blue (Biotool, LLC; B34102) at 37°C for 4 h, and fluorescent intensity was measured at Ex 535 nm/Em 595 nm. Then, the cells were cultured with fresh medium until the next round of measurement. Means and standard deviation (SDs) of triplicate measurements were calculated and plotted.

RNA isolation and TaqMan-quantitative reverse transcription PCR (qRT-PCR) analysis. Total RNA was isolated from cells at the logarithmic phase by using TRIzol reagent (Tiangen Biotech Co., Ltd., Beijing, China). Steady states of target and β -actin mRNA levels were simultaneously quantified by dual-qRT-PCR assay with differentially fluorescent-labeled TaqMan probes for the target (Cy5 or Rox) and β -actin mRNA (HEX) (ShingGene, Shanghai, China). An FTC-3000P PCR instrument (Funglyn Biotech Inc., Richmond Hill, ON, Canada) was employed in the process. For miR analysis, cDNA was synthesized with the specific stem-loop primer and quantified by TaqMan-qRT-PCR assay. Through the $2^{-\Delta\Delta Ct}$ method, U6 reads were normalized for miR or with β -actin for mRNA. The primer and probe sequences were: hNET1 F, 5'-AGCCAA GCAATAAAAGAGTTCG-3'; hNET1 R, 5'-GGTCACCAC GAAGGGTAAATG-3' and hNET1 probe, 5'-ROX-CACGTC CTTGGCAAATTTAATCTCTCCTG-3'; hACTB F, 5'-GCC CATCTACGAGGGGTATG-3'; hACTB R, 5'-GAGGTA GTCAGTCAGGTCCTG-3' and hACTB probe, 5'-HEX-CCC CCATGCCATCCTGCGTC-3'; miR-22-3p RT, 5'-GCGCGT GAGCAGGCTGGAGAAATTAACCACGCGCACAGTT-3'; miR-22-3p R, 5'-GAGCAGGCTGGAGAA-3'; miR-22-3p F, 5'-GGAAGCTGCCAGTTGA-3' and miR-22-3p probe, 5'-cy5-CCACGCGCACAGTTC-3'; U6 RT, 5'-GTCGTATCC AGTGCAGGGTCCGAGGTATTCGCACTGATACGACAA AAATATG-3'; U6 F, 5'-GCTTCGGCAGCACATA-3'; U6 R, 5'-CTTCACGAATTTGCGTG-3' and U6 probe, 5'-HEX-CCT TGCGCAGGGGCCATGC-MGB3'.

Western blot analysis. Cells at the logarithmic phase of culture were lysed in a solution of 60 mM Tris-HCl (pH 6.8), 2% sodium dodecyl sulphate, 20% glycerol, 0.25% bromophenol blue and 1.25% 2-mercaptoethanol and then heated at 100°C for 10 min before electrophoresis and western blot analysis. Anti-NET1 antibody (1:1,000; cat. no. 12740-1-AP), anti-glyceraldehyde-3-phosphate dehydrogenase (GAPDH) antibody (1:1,000; cat. no. 60004-1-Ig), anti-rabbit IgG peroxidase-conjugated antibody (1:1,000; cat. no. SA00001-2) and horseradish peroxidase-conjugated goat anti-mouse IgG antibody (1:1,000; cat. no. SA00001-1) employed in the study were purchased from Proteintech Group, Inc. (Chicago, IL, USA).

Target bands were revealed by enhanced chemiluminescence reaction (Pierce, Rockford, IL, USA), and relative density of each protein over GAPDH was quantified using Gel-Pro Analyser (Media Cybernetics, Inc., Rockville, MD, USA).

Colony formation assay. After 24 h of transfection, 2000 transfected cells were placed in fresh 6-well plates in triplicate and maintained in RPMI-1640 medium containing 10% FBS. The medium was replaced every 3 days, and samples were incubated for 2 weeks at 37°C and under 5% CO_2 in an incubator. Colony formation was observed with the naked eye to determine the time for termination of experiments. Clones were then fixed with methanol, stained with 0.1% crystal violet for 30 min and then counted and recorded.

Cell apoptosis analysis. Apoptosis was analysed by Annexin V/propidium iodide (PI) double staining. After transfection for 48 h, cells in the logarithmic growth phase were harvested and rinsed twice with ice-bathed PBS. Afterward, fluorescein isothiocyanate-labeled enhanced Annexin V (3 μ l) and PI (3 μ l) were added to the cell suspension at a final volume of 150 μ l. After incubation for 30 min, flow cytometry was performed on a FACSCalibur instrument (BD Biosciences, San Jose, CA, USA). The numbers of apoptotic and necrotic cells were calculated by flow cytometry (Becton-Dickinson, San Jose, CA, USA) and analysed by FlowJo v10 software (FlowJo LLC, Ashland, OR, USA). Ratio of early apoptosis was adopted for the test results. Experiments were independently performed thrice, and a representative was subsequently obtained.

Statistical analysis. Data are presented as means, and error bars indicate SD or standard error (SE) around the mean. All statistical analyses were performed with GraphPad Prism v.6.0 (GraphPad Software, Inc., La Jolla, CA, USA). Two-tailed Student's t-test, one-way ANOVA or Mann-Whitney U test was employed to calculate for statistical significance. $P < 0.05$ was considered to indicate statistically significant differences.

Results

miR-22-3p levels were higher in chemoresistant (H-bc) than in chemosensitive (5637) BCa cell lines. Based on the fold differences of relative chemoresistance indices (average of relative IC_{50} to each drug) of BCa cell lines to seven chemotherapeutics (Pi, Pa, Ad, EH, Ci, Hy and Ge), 5637 was the most multi-chemosensitive, whereas H-bc was the most multi-chemoresistant cell line (Table I). 5637 and H-bc have been reported as relatively multi-chemosensitive and multi-chemoresistant BCa cell lines, respectively (10-13). As revealed by both sequencing-based miR-omic analysis (miR-omic: 1.00:10.10; Fig. 1A) and qRT-PCR validation (qRT-PCR: 1.00:18.52; Fig. 1B), miR-22-3p level was over 18-fold higher in H-bc than in 5637 cells (Fig. 1B). All these observations suggest that miR-22-3p may promote BCa chemoresistance similar to miR-193a-3p (10).

NET1 mRNA is a target of miR-22-3p in BCa cells. To understand multiple chemoresistance mechanisms of miR-22-3p-regulated BCa, we first used the bioinformatic

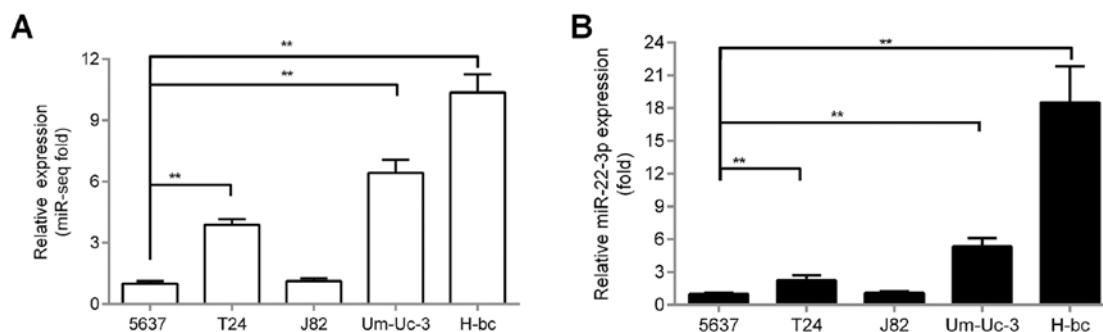


Figure 1. miR-22-3p expression is upregulated in multidrug-resistant BCa cells. Relative miR-22-3p levels (fold) in five BCa cell lines as determined by miR-seq (A) and qRT-PCR analyses (B) are shown in the plot. ** $P < 0.01$.

Table I. Chemo-resistance (IC_{50}) to each drug in the BCa cell lines.

Agents	Relative IC_{50} values of the cell lines				
	5637	T24	J82	Um-Uc-3	H-bc
Pi	1.00	3.39	5.36	3.68	9.65
Pa	1.00	13.67	18.52	13.51	16.24
Ad	1.00	3.08	2.67	8.83	9.32
EH	1.00	1.74	25.22	22.05	37.96
Hy	1.00	1.18	2.85	1.85	120.82
Ci	1.00	1.18	1.77	1.02	1.71
Ge	3.88	1.00	3.19	15.94	3578
Chemo-resistance index	1.41	3.61	8.51	9.55	539.10

Relative IC_{50} (fold) values normalized to the lowest IC_{50} are presented. Chemo-resistance indices (average of relative IC_{50} to each drug) of cell lines are also displayed. Pi, pirarubicin; Pa, paclitaxel; Ad, Adriamycin; EH, epirubicin hydrochloride; Hy, hydroxycamptothecin; Ci, cisplatin; Ge, gemcitabine.

software miRDB and TargetScan to perform bioinformatic analysis. We studied 240 target genes that appeared simultaneously in the two predictive softwares and some target genes of miR-22-3p that have been studied; these target genes of miR-22-3p include *TET2* (18), *NET1* (25), *CD147* (20), *Tcf7* (26), *VE-cadherin* (27), *TGF β R* (28), *KDM3A* (21), *CD151* (16), *MTHFR* (15), *HMGB1* (22), *Sp1* (29) and *SRF* (30) (only some of the genes appeared among the 240 target genes predicted by the website). These genes were detected by RNA-seq in 5637 and H-bc cell lines to identify the target of miR-22-3p in BCa. Among the two cell lines, NET1 was the more pronounced target gene, and its expression was opposite to that of miR-22-3p. qRT-PCR and western blot analysis indicated that NET1 levels, including mRNA (RNA-seq analysis: 1.00:0.15 and qRT-PCR analysis: 1.00:0.25; Fig. 2B) and protein levels (western blot analysis: 1.00:0.50; Fig. 2A), were significantly higher in 5637 than in H-bc cells.

Given our above-mentioned studies, we observed that NET1 and miR-22-3p levels are negatively correlated. Hence, miR-22-3p may function by regulating NET1 expression to

influence BCa chemoresistance. To further detect whether NET1 is a genuine target gene of miR-22-3p in BCa, we examined mRNA expression of NET1 in 5637 and H-bc cells transfected with miR-22-3p mimic (3PM) and miR-22-3p antagomir (3PA), respectively, vs. NC. qRT-PCR results revealed that the expression of miR-22-3p-mimic-transfected 5637 cells increased by >37-fold vs. that of NC (Fig. 3A). By contrast, miR-22-3p expression was significantly reduced by 78.0% in the miR-22-3p-antagomiR-transfected H-bc cells vs. NC (Fig. 3A). As expected, miR-22-3p mimic transfection decreased NET1 mRNA levels by 50.8% and protein levels by 47.74% with respect to those of NC in 5637 cells (Fig. 3B and C). Similarly, miR-22-3p antagomiR transfection increased NET1 mRNA levels by 64.0% and protein levels by 2.29 times that of NC in H-bc cells (Fig. 3B and C).

To confirm whether NET1 is a target gene of miR-22-3p in BCa, we demonstrated that the 3'UTR region of NET1 contains a potential binding region of miR-22-3p (150-157 bp) by sequence analysis (Fig. 3D). We placed wild-type (wt) and mutant (mut) NET1 genes downstream the luciferase gene of the control vector (pGL3-vector; Promega) to produce PGL3-NET1-UTR-wt/mut (Fig. 3D). These constructs and control vector (PGL3-vector) were transfected into 5637 and H-bc cells, respectively, for comparison of luciferase activities. As shown in Fig. 3E and F, in mimic-transfected 5637 cells, PGL3-NET1-UTR-wt exhibited lower luciferase activity than the other two reported constructs with respect to that of the NC. By contrast, activities in antagomiR-transfected H-bc cells were higher. In conclusion, our findings strongly indicated that NET1 is a target of miR-22-3p in BCa.

NET1 negatively correlates with the promotive effect of miR-22-3p on BCa multi-chemoresistance. To investigate whether inhibition and overexpression of NET1 produces steady effects with miR-22-3p mimic/antagomiR, we designed, synthesized and transfected NET1 siRNA into 5637 cells. Simultaneously, we constructed a NET1 overexpression vector (pINDUCER21-EGFP-NET1) by using the plasmid of tetracycline-induced expression system with green fluorescent protein and transfected this plasmid into H-bc cells. Protein and mRNA levels of NET1 were downregulated by transfection of si-NET1 (western blot analysis: 0.12:1.00; qRT-PCR: 0.36:1.00; Fig. 4A and B). This finding was consistent with that of miR-22-3p mimic transfection (western blot analysis: 0.42:1.00; qRT-PCR: 0.51:1.00; Fig. 3B and C) in 5637 cells with respect

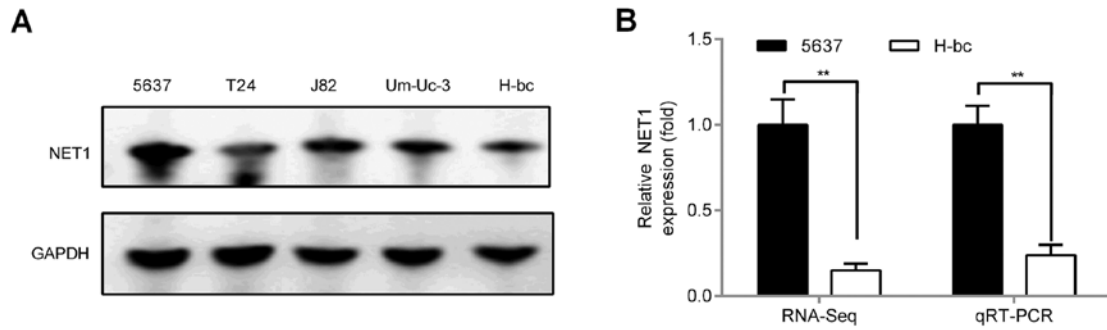


Figure 2. NET1 levels are higher in 5637 than in H-bc cells. (A) Western blot analysis determined the relative protein levels (fold) of the NET1 gene in BCa cells. (B) Relative mRNA levels (fold) of the NET1 gene in 5637 and H-bc cells were analyzed by miR-seq and qRT-PCR analyses and are illustrated in the plot. **P<0.01.

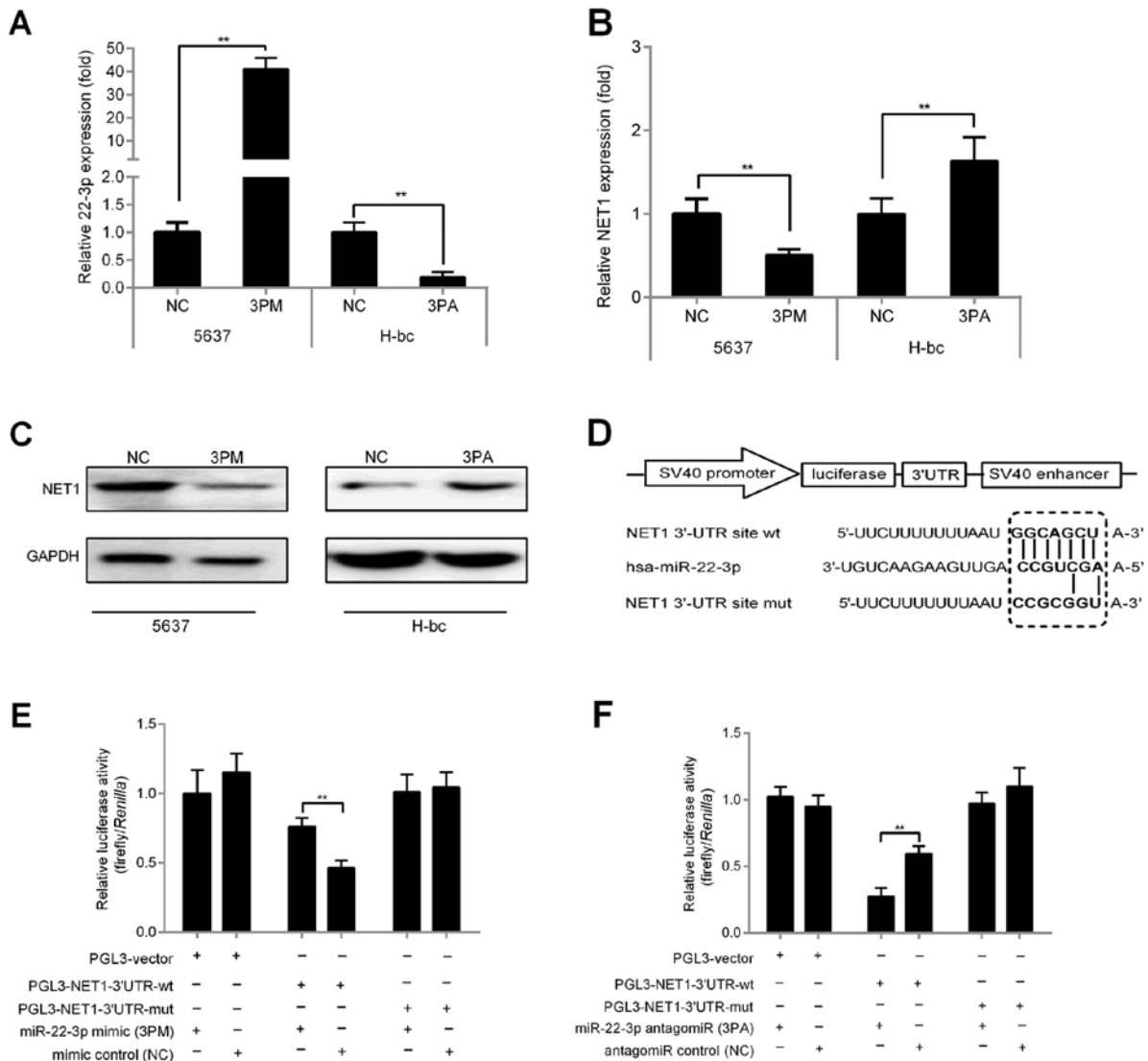


Figure 3. NET1 is a novel target of miR-22-3p in BCa cells. (A) miR-22-3p level and (B) NET1 mRNA and (C) protein levels, as determined by qRT-PCR or western blot analyses in miR-22-3p-mimic-transfected (3PM) 5637 cells and miR-22-3p-antagomiR-transfected (3PA) H-bc cells, are compared against the results of NC. (D) A putative binding site for miR-22-3p in the 3'UTR of NET1 mRNA is shown, and mutation (dashed box and bold) within the binding site is generated. Relative luciferase activity (fold) of the reporter with WT or Mut NET1-UTR or without UTR (Vec) were determined in (E) miR-22-3p mimic (in 5637) or (F) antagomiR (in H-bc). *Renilla* luciferase activity of a co-transfected control plasmid was used to control transfection efficacy. Representative results from three independent experiments are presented. Error bars represent SD of triplicate samples. **P<0.01.

to that of NC. Cell death triggered by all six drugs (Pi, Pa, Ad, EH, Ci and Hy, but not Ge) was significantly attenuated

after transfection with miR-22-3p mimic (Fig. 4C), whereas cell death caused by Pi, Pa, Ad and Ci was significantly

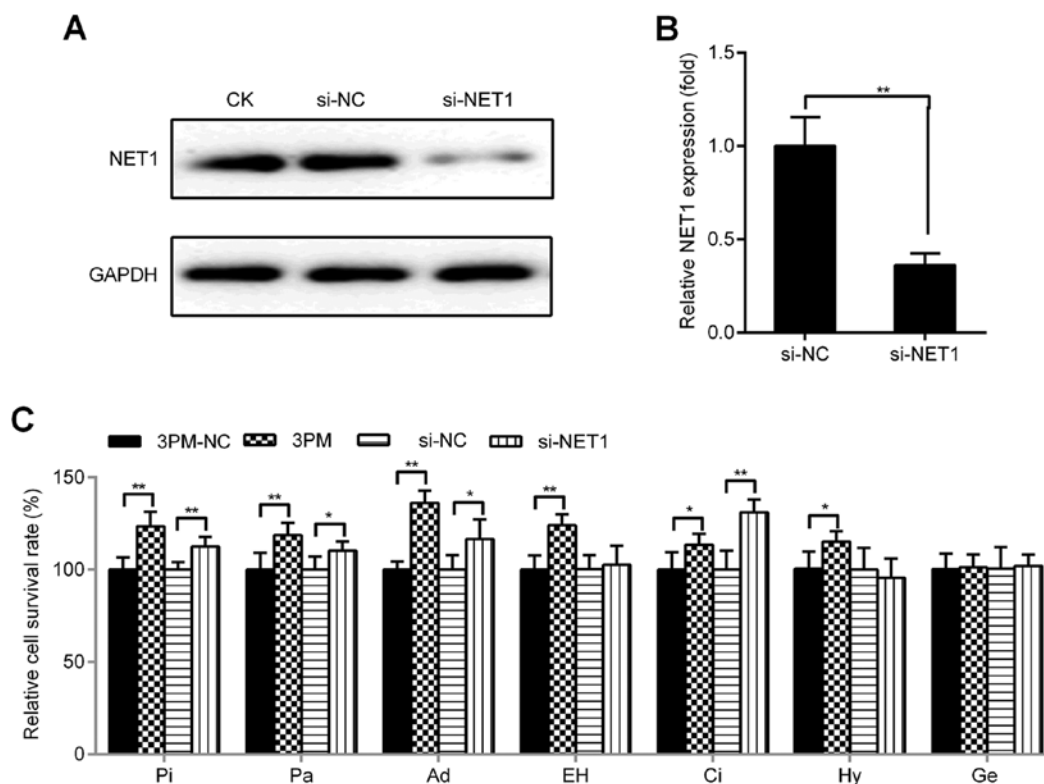


Figure 4. Effects of forced reversal of miR-22-3p or NET1 levels on multi-drug resistance of 5637 cells. (A) NET1 protein level (western blot analysis) and (B) mRNA level (qRT-PCR) in si-NET1-transfected cells were compared against NC-transfected 5637 cells and control check (CK). (C) Relative cell survival of 5637 cells transfected with 3PM or si-NET1 are compared with the respective control groups (3PM-NC and si-NC-transfected 5637 cells) 72 h after treatment with IC₅₀-dose drugs. *P<0.05, **P<0.01. 3PM, miR-22-3p-mimic-transfected 5637 cells. Pi, pirarubicin; Pa, paclitaxel; Ad, Adriamycin; EH, epirubicin hydrochloride; Hy, hydroxycamptothecin; Ci, cisplatin; Ge, gemcitabine.

attenuated after transfection with NET1 siRNA with respect to those of NC (Fig. 4C). Conversely, EGFP-NET1 was used for transfection and successfully induced with docetaxel in H-bc cells (Fig. 5A), where NET1 protein and mRNA levels were upregulated (western blot analysis: 2.14:1.00; qRT-PCR: 3.06:1.00; Fig. 5B and C, respectively). H-bc became further amenable to cell death triggered by Pi, Pa and Ci (Fig. 5D). Similar to EGFP-NET1 transfection, miR-22-3p antagonism transfection sensitized H-bc cells to Pi, Pa, Ad, Ci and Hy but not to EH and Ge (Fig. 5D).

Forced reversal of miR-22-3p and NET1 on colony formation and apoptosis in chemoresistant BCa cells. We then investigated whether miR-22-3p is involved in colony formation and apoptosis of BCa cells in H-bc and 5637 cells. miR-22-3p mimic or si-NET1 was transfected into 5637 cells to detect colony formation and apoptosis. Compared with the control cells, miR-22-3p-mimic- or si-NET1-transfected cells significantly increased the number of cell colonies and decreased the number of apoptotic cells (Figs. 6A and 7A). We then transfected miR-22-3p antagonism or overexpressed EGFP-NET1 into H-bc cells and performed the same experiment. The results revealed a decreased number of colonies and increased apoptotic rate in the H-bc cells (Figs. 6B and 7B). miR-22-3p possibly enhanced colonies formation of BCa cells and inhibited cell apoptosis by modulating the NET1 gene. Overall, the NET1 gene contributed significantly in promoting miR-22-3p-mediated tolerance to BCa chemotherapy.

Discussion

Tumor resistance to chemotherapy is a key reason underlying the poor prognosis of patients with clinical cancer. With the increase in the research of the association of miRNAs and tumor behavior, an increasing number of studies have revealed information in regards to the abnormal expression of miRNAs and clinical chemotherapy drug tolerance. miRNA mutations, abnormal expression or abnormal processing affect the normal functions of miRNAs and lead to ectopic expression of target proteins. When target genes in tumor cells are regulated by miRNAs, the sensitivity of tumor cells to drug changes. Studies have shown that miR-22 affects chemotherapeutic tolerance of osteosarcoma cells by regulating its target gene HMGB1 (22). However, understanding the role of miR-22-3p in cancer chemoresistance, especially in BCa, remains elusive.

In BCa, a new panel of miR-22-3p-targeting genes may play pivotal roles in multi-drug chemoresistance of BCa. We identified bioinformatic-predicted target genes at the RNA-seq omic level in multi-chemosensitive 5637 and multi-chemoresistant H-bc cells which exhibited differential expression of miR-22-3p. Results were then verified by qRT-PCR of the target gene (Figs. 1 and 2). Findings indicated that NET1 levels were significantly higher in 5637 cells than in H-bc cells and were negatively correlated with miR-22-3p expression. Subsequently, we revealed that NET1 is a direct target gene of miR-22-3p and plays a catalytic role in BCa chemoresistance (Figs. 3-7). In colon cancer/gastric cancer, NET1 was also found to be a

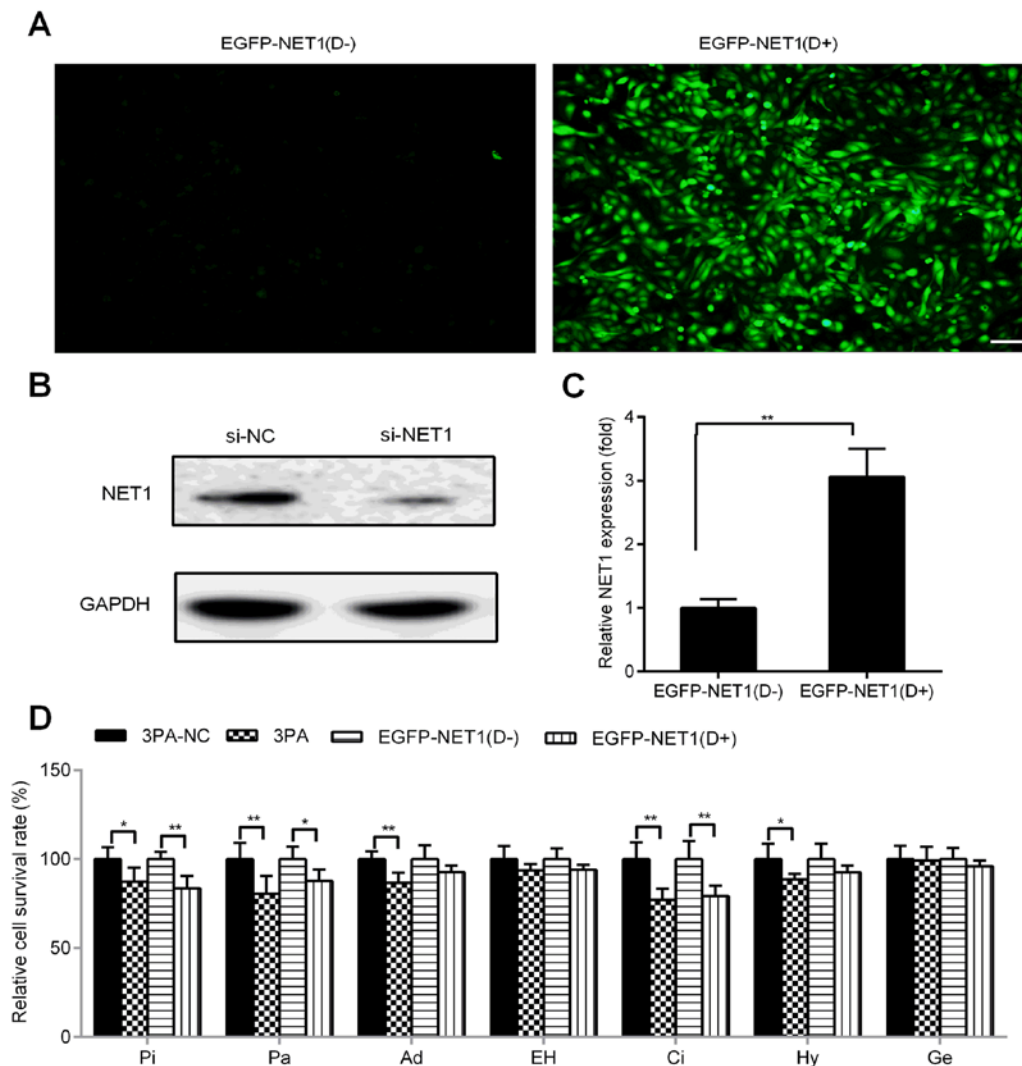


Figure 5. Effects of forced reversal of miR-22-3p or NET1 levels on multi-drug resistance of H-bc cells. (A) NET1 expression in overexpression-construct-transfected H-bc cells are displayed. Representative areas of H-bc cells transfected with EGFP-NET1(D+) (added doxycycline) are compared with those of cells transfected with EGFP-NET1(D-) (without doxycycline). Scale bar, 50 μ m. (B) NET1 protein level (western blot analysis) and (C) mRNA level (qRT-PCR) in EGFP-NET1(D+)-transfected H-bc cells are compared with that in EGFP-NET1(D-)-transfected H-bc counterparts. (D) Relative cell survival of H-bc cells transfected with miR-193a-3p antagonist (3PA) or EGFP-NET1(D+) are compared against respective control groups (3PA-NC- and EGFP-NET1(D-)-transfected H-bc cells) 72 h after treatment with IC_{50} -dosed drugs. * $P < 0.05$, ** $P < 0.01$. Pi, pirarubicin; Pa, paclitaxel; Ad, Adriamycin; EH, epirubicin hydrochloride; Hy, hydroxycamptothecin; Ci, cisplatin; Ge, gemcitabine.

target gene of miR-638/miR-573 (31,32). The above-mentioned study indicated that miR-22-3p plays a similar role to that of miR-193a-3p in BCa chemoresistance (10).

NET1 is among the seven members of the transmembrane 4 superfamily (TM4SF), which was discovered by Serru *et al* in the EST database (33). NET1 is located on chromosome 1p34.1 and features a total length of 1297 bp, a coding sequence of 128-853 bp, a 241-amino-acid ORF (GenBank accession no. NM005727.3), which are typical structural characteristics of TM4SF. The amino acid sequence of NET1 is homologous to those of other TM4SF members by 36% (CD82), 32% (CO-029) and 29% (Talla-1). NET1 mediates extracellular signal transduction through cysteine residues in its transmembrane domain (34). Previous studies have shown that NET1 is a novel tumor-related gene associated with many malignancies, including hepatocellular carcinoma (35), skin squamous cell carcinoma (SSCC) (36), breast (37), colorectal (31), lung (38) and gastric cancer (32).

NET1 knockout was found to reduce the proliferation, invasion and tumor growth of SSCC cells (36). NET1 gene overexpression in breast adenocarcinoma cell lines also led to excessive cell migration (37). NET1 is related to chemoresistance in BCa through a highly complex mechanism. Hence, we investigated the drug resistance mechanism of the NET1 gene in BCa cells. Reversal of NET1/miR-22-3p expression in 5637 cells inhibited cell death triggered by each of the six drugs used in the present study except for gemcitabine (Fig. 4C). Similarly, reversing expression of NET1/miR-22-3p in H-bc cells promotes drug-triggered cell death except for epirubicin hydrochloride and gemcitabine (Fig. 5D). This result indicated that the influence of miR-22-3p/NET1 on the drug resistance of different drugs may not be consistent among different types of tumor cells due to heterogeneity. Therefore, understanding the role of miR-22-3p/NET1 in the sensitivity of different drugs and different types of tumors is crucial for its future clinical application.

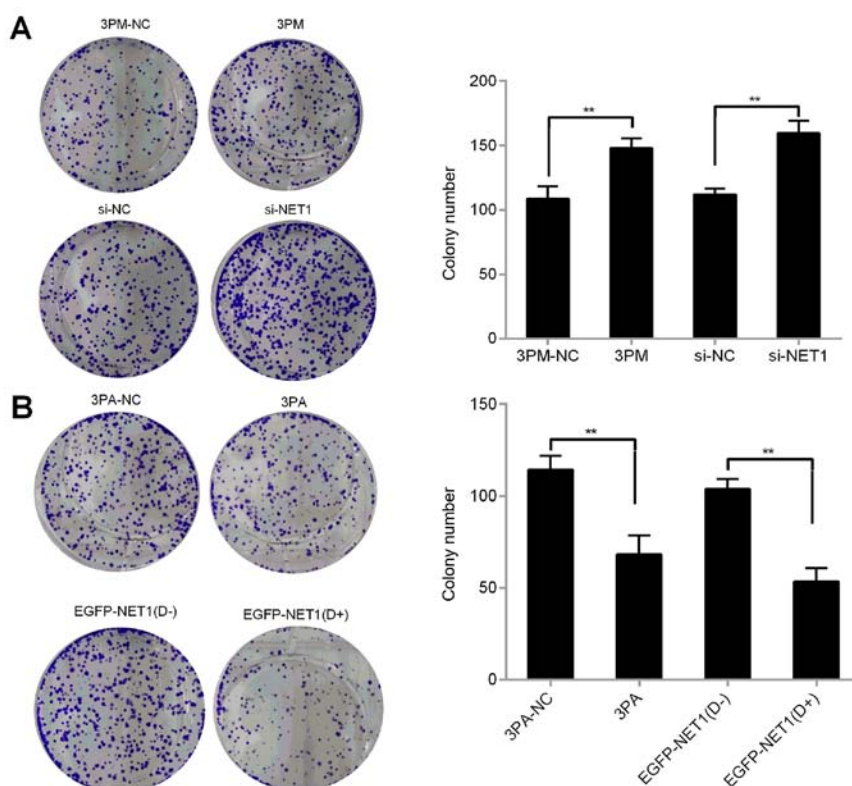


Figure 6. Effects of forced reversal of miR-22-3p or NET1 levels on plate colony formation assay. (A) Effects of forced reversal with transient expression of 3PM, si-NET1 and corresponding NC on plate colony formation assay results of 5637 cells are presented. A graph of the representative original and plotted results are shown. (B) Effects of forced reversal with transient expression of 3PA, EGFP-NET1 and corresponding NC on plate colony formation assay of H-bc cells are also displayed through a representative original and plotted results. ** $P < 0.01$. 3PM, miR-22-3p-mimic-transfected 5637 cells; 3PA, miR-22-3p-antagomiR-transfected H-bc cells; (D+), added doxycycline; (D-), without doxycycline.

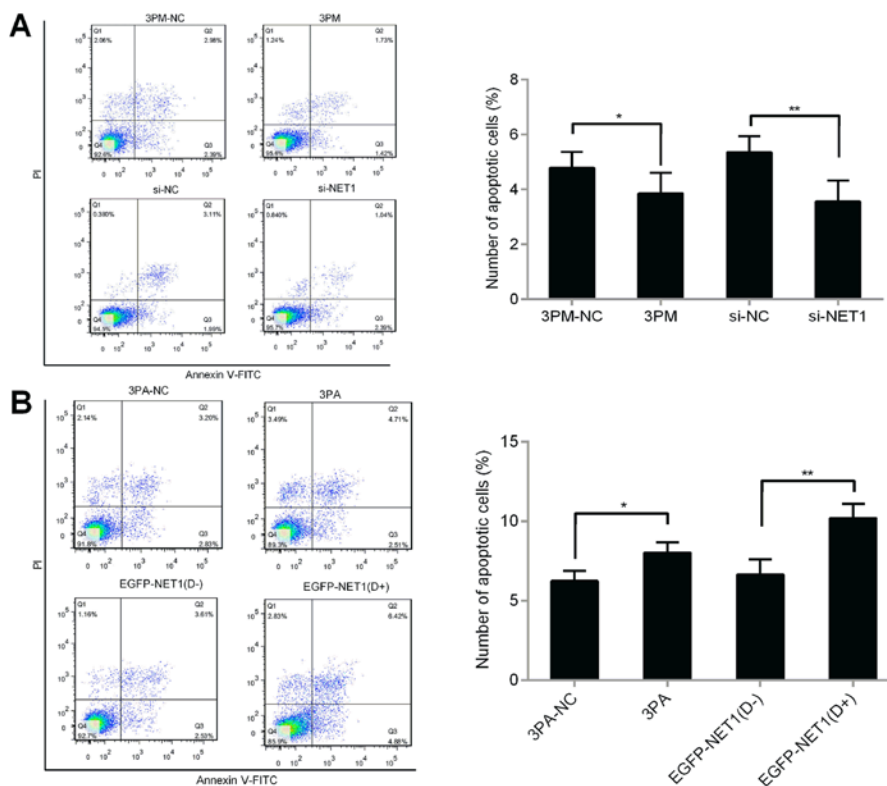


Figure 7. Effects of forced reversal of miR-22-3p or NET1 levels on apoptosis. (A) Effects of forced reversal with transient expression of 3PM, si-NET1 and corresponding NC on apoptosis assay results of 5637 cells are presented. A graph of the representative original FACS data and plotted results are shown. (B) Effects of forced reversal with transient expression of 3PA, EGFP-NET1 and corresponding NC on apoptosis assay of H-bc cells are also displayed through a representative original FACS data and plotted results are shown. * $P < 0.05$, ** $P < 0.01$. 3PM, miR-22-3p-mimic-transfected 5637 cells; 3PA, miR-22-3p-antagomiR-transfected H-bc cells; (D+), added doxycycline; (D-), without doxycycline.

As indicated above, NET1 exerts carcinogenic effects and may play a fundamental role in cancer development. However, the role of NET1 in BCa has been only slightly studied. In the present study, our data found that si-NET1 restrained expression of NET1 and consequently inhibited BCa apoptosis and promoted colony formation. miR-22-3p mimic exerted the same effect in 5637 cells (Figs. 6A and 7A). Successful induction of the NET1 overexpression vector with green fluorescent protein and a tetracycline-inducing system resulted in NET1 overexpression, which then promoted BCa apoptosis and inhibited colony formation. miR-22-3p antagonist exerted the same effect on H-bc cells (Figs. 6B and 7B). These results demonstrated that miR-22-3p-mediated NET1 regulation may promote BCa chemoresistance. In the past few years, the research on molecular mechanism of apoptosis made breakthrough progress. It has been shown that many apoptosis-related genes participate in apoptotic processes, including caspases, death receptors and Bcl-2. The role of these genes on the miR-22-3p signal axis in BCa chemoresistance awaits further research.

In conclusion, miR-22-3p expression induces chemoresistance in BCa cell lines. miR-22-3p may partially promote chemotherapeutic tolerance by targeting NET1. Thus, miR-22-3p and NET1 may serve as predictive chemopathic markers for BCa patients. The detailed mechanism of BCa chemoresistance through miR-22-3p-regulated NET1 targeting must be explored, and further studies on cell signaling and *in vitro* nude mouse-transplanted tumor systems will be conducted.

Acknowledgements

Not applicable.

Funding

The present study was supported by the National Natural Science Foundation of China (nos. 81502191 and 81702540) and the Anhui Provincial Natural Science Foundation (nos. 1608085MH166, 1508085QH178, 1508085QH183, 1708085QH202 and 1708085QH179).

Availability of data and materials

The datasets are available from Dr Tao Tao upon reasonable request.

Authors' contributions

TT and JX conceived and designed the study. SN, JX, JZ, DP, DS, CX and HD performed the experiments. SN and LL wrote the manuscript. TT, ZS and JX reviewed and edited the manuscript. All authors read and approved the manuscript and agree to be accountable for all aspects of the research in ensuring that the accuracy or integrity of any part of the work are appropriately investigated and resolved.

Ethics approval and consent to participate

This study did not involve human participants and animals.

Consent for publication

This study did not involve human participants.

Competing interests

The authors declare that they have no competing interests.

References

1. Siegel RL, Miller KD and Jemal A: Cancer statistics, 2017. *CA Cancer J Clin* 67: 7-30, 2017.
2. Chang JS, Lara PN Jr and Pan CX: Progress in personalizing chemotherapy for bladder cancer. *Adv Urol* 2012: 364919, 2012.
3. Bambury RM, Power DG and O'Reilly S: Intratumor heterogeneity and branched evolution. *N Engl J Med* 366: 2132-2133, 2012.
4. Setoyama T, Ling H, Natsugoe S and Calin GA: Non-coding RNAs for medical practice in oncology. *Keio J Med* 60: 106-113, 2011.
5. Chan B, Manley J, Lee J and Singh SR: The emerging roles of microRNAs in cancer metabolism. *Cancer Lett* 356: 301-308, 2015.
6. Allen KE and Weiss GJ: Resistance may not be futile: microRNA biomarkers for chemoresistance and potential therapeutics. *Mol Cancer Ther* 9: 3126-3136, 2010.
7. Vinall RL, Ripoll AZ, Wang S, Pan CX and deVere White RW: MiR-34a chemosensitizes bladder cancer cells to cisplatin treatment regardless of p53-Rb pathway status. *Int J Cancer* 130: 2526-2538, 2012.
8. Tao J, Lu Q, Wu D, Li P, Xu B, Qing W, Wang M, Zhang Z and Zhang W: microRNA-21 modulates cell proliferation and sensitivity to doxorubicin in bladder cancer cells. *Oncol Rep* 25: 1721-1729, 2011.
9. Su SF, Chang YW, Andreu-Vieyra C, Fang JY, Yang Z, Han B, Lee AS and Liang G: miR-30d, miR-181a and miR-199a-5p cooperatively suppress the endoplasmic reticulum chaperone and signaling regulator GRP78 in cancer. *Oncogene* 32: 4694-4701, 2013.
10. Lv L, Li Y, Deng H, Zhang C, Pu Y, Qian L, Xiao J, Zhao W, Liu Q, Zhang D, *et al*: MiR-193a-3p promotes the multi-chemoresistance of bladder cancer by targeting the HOXC9 gene. *Cancer Lett* 357: 105-113, 2015.
11. Deng H, Lv L, Li Y, Zhang C, Meng F, Pu Y, Xiao J, Qian L, Zhao W, Liu Q, *et al*: The miR-193a-3p regulated *PSEN1* gene suppresses the multi-chemoresistance of bladder cancer. *Biochim Biophys Acta* 1852: 520-528, 2015.
12. Deng H, Lv L, Li Y, Zhang C, Meng F, Pu Y, Xiao J, Qian L, Zhao W, Liu Q, *et al*: miR-193a-3p regulates the multi-drug resistance of bladder cancer by targeting the LOXL4 gene and the oxidative stress pathway. *Mol Cancer* 13: 234, 2014.
13. Li Y, Deng H, Lv L, Zhang C, Qian L, Xiao J, Zhao W, Liu Q, Zhang D, Wang Y, *et al*: The miR-193a-3p-regulated ING5 gene activates the DNA damage response pathway and inhibits multi-chemoresistance in bladder cancer. *Oncotarget* 6: 10195-10206, 2015.
14. Gurha P, Abreu-Goodger C, Wang T, RamiRez MO, Drumond AL, van Dongen S, Chen Y, Bartonicek N, Enright AJ, Lee B, *et al*: Targeted deletion of microRNA-22 promotes stress-induced cardiac dilation and contractile dysfunction. *Circulation* 125: 2751-2761, 2012.
15. Li C, Ni J, Liu YX, Wang H, Liang ZQ and Wang X: Response of MiRNA-22-3p and MiRNA-149-5p to folate deficiency and the differential regulation of *MTHFR* expression in normal and cancerous human hepatocytes. *PLoS One* 12: e0168049, 2017.
16. Wang X, Yu H, Lu X, Zhang P, Wang M and Hu Y: MiR-22 suppresses the proliferation and invasion of gastric cancer cells by inhibiting CD151. *Biochem Biophys Res Commun* 445: 175-179, 2014.
17. Song SJ, Polisen L, Song MS, Ala U, Webster K, Ng C, Beringer G, Brikbak NJ, Yuan X, Cantley LC, *et al*: MicroRNA-antagonism regulates breast cancer stemness and metastasis via TET-family-dependent chromatin remodeling. *Cell* 154: 311-324, 2013.

18. Song SJ, Ito K, Ala U, Kats L, Webster K, Sun SM, Jongen-Lavrencic M, Manova-Todorova K, Teruya-Feldstein J, Avigan DE, *et al*: The oncogenic microRNA miR-22 targets the TET2 tumor suppressor to promote hematopoietic stem cell self-renewal and transformation. *Cell Stem Cell* 13: 87-101, 2013.
19. Polisenio L, Salmena L, Riccardi L, Fornari A, Song MS, Hobbs RM, Sportoletti P, Varmeh S, Egia A, Fedele G, *et al*: Identification of the *miR-106b~25* microRNA cluster as a proto-oncogenic *PTEN*-targeting intron that cooperates with its host gene *MCM7* in transformation. *Sci Signal* 3: ra29, 2010.
20. Luo LJ, Zhang LP, Duan CY, Wang B, He NN, Abulimiti P and Lin Y: The inhibition role of miR-22 in hepatocellular carcinoma cell migration and invasion via targeting CD147. *Cancer Cell Int* 17: 17, 2017.
21. Parrish JK, Sechler M, Winn RA and Jedlicka P: The histone demethylase KDM3A is a microRNA-22-regulated tumor promoter in Ewing Sarcoma. *Oncogene* 34: 257-262, 2015.
22. Li X, Wang S, Chen Y, Liu G and Yang X: miR-22 targets the 3'UTR of HMGB1 and inhibits the HMGB1-associated autophagy in osteosarcoma cells during chemotherapy. *Tumour Biol* 35: 6021-6028, 2014.
23. Bennett G, Sadlier D, Doran PP, Macmathuna P and Murray DW: A functional and transcriptomic analysis of NET1 bioactivity in gastric cancer. *BMC Cancer* 11: 50, 2011.
24. He S, Wei YZ, Wang GL, Xu YY, Zhou JM, Zhang YX and Chen L: Study of RNA interference targeting NET-1 combination with sorafenib for hepatocellular carcinoma therapy in vitro and in vivo. *Gastroenterol Res Pract* 2013: 685150, 2013.
25. Ahmad HM, Muiwo P, Ramachandran SS, Pandey P, Gupta YK, Kumar L, Kulshreshtha R and Bhattacharya A: miR-22 regulates expression of oncogenic neuro-epithelial transforming gene 1, NET1. *FEBS J* 281: 3904-3919, 2014.
26. Kaur K, Vig S, Srivastava R, Mishra A, Singh VP, Srivastava AK and Datta M: Elevated hepatic miR-22-3p expression impairs gluconeogenesis by silencing the wnt-responsive transcription factor Tcf7. *Diabetes* 64: 3659-3669, 2015.
27. Gu W, Zhan H, Zhou XY, Yao L, Yan M, Chen A, Liu J, Ren X, Zhang X, Liu JX and Liu G: MicroRNA-22 regulates inflammation and angiogenesis via targeting VE-cadherin. *FEBS Lett* 591: 513-526, 2017.
28. Hong Y, Cao H, Wang Q, Ye J, Sui L, Feng J, Cai X, Song H, Zhang X and Chen X: MiR-22 may suppress fibrogenesis by targeting TGFbetaR I in cardiac fibroblasts. *Cell Physiol Biochem* 40: 1345-1353, 2016.
29. Chen J, Wu FX, Luo HL, Liu JJ, Luo T, Bai T, Li LQ and Fan XH: Berberine upregulates miR-22-3p to suppress hepatocellular carcinoma cell proliferation by targeting Spl. *Am J Transl Res* 8: 4932-4941, 2016.
30. Xu D, Guo Y, Liu T, Li S and Sun Y: miR-22 contributes to endosulfan-induced endothelial dysfunction by targeting SRF in HUVECs. *Toxicol Lett* 269: 33-40, 2017.
31. Zhang J, Fei B, Wang Q, Song M, Yin Y, Zhang B, Ni S, Guo W, Bian Z, Quan C, *et al*: MicroRNA-638 inhibits cell proliferation, invasion and regulates cell cycle by targeting tetraspanin 1 in human colorectal carcinoma. *Oncotarget* 5: 12083-12096, 2014.
32. Lu Z, Luo T, Nie M, Pang T, Zhang X, Shen X, Ma L, Bi J, Wei G, Fang G and Xue X: TSPAN1 functions as an oncogene in gastric cancer and is downregulated by miR-573. *FEBS Lett* 589: 1988-1994, 2015.
33. Serru V, Dessen P, Boucheix C and Rubinstein E: Sequence and expression of seven new tetraspans. *Biochim Biophys Acta* 1478: 159-163, 2000.
34. Todres E, Nardi JB and Robertson HM: The tetraspanin superfamily in insects. *Insect Mol Biol* 9: 581-590, 2000.
35. Ye K, Chang S, Li J, Li X, Zhou Y and Wang Z: A functional and protein-protein interaction analysis of neuroepithelial cell transforming gene 1 in hepatocellular carcinoma. *Tumour Biol* 35: 11219-11227, 2014.
36. zhang J, Wang J, Chen L, Wang G, Qin J, Xu Y and Li X: Expression and function of NET-1 in human skin squamous cell carcinoma. *Arch Dermatol Res* 306: 385-397, 2014.
37. Ecimovic P, Murray D, Doran P and Buggy DJ: Propofol and bupivacaine in breast cancer cell function in vitro-role of the *NET1* gene. *Anticancer Res* 34: 1321-1331, 2014.
38. Fang L, Zhu J, Ma Y, Hong C, Xiao S and Jin L: Neuroepithelial transforming gene 1 functions as a potential prognostic marker for patients with non-small cell lung cancer. *Mol Med Rep* 12: 7439-7446, 2015.